Hyperfine Interact (2016) 237:110
DOI 10.1007/s10751-016-1322-5

# Mössbauer study of iron carbide nanoparticles produced by laser ablation in alcohols

**S. Amagasa[1] · N. Nishida[1] · Y. Kobayashi[2,3] · Y. Yamada[1]**



**Abstract** Iron carbide nanoparticles were synthesized by laser ablation of iron in alcohols (methanol and ethanol). A new cell, designed to allow the ablation to be conducted in a flowing solvent, enabled separation and collection of the nanoparticles immediately after production, thus preventing further photochemical reactions of the colloids. The nanoparticles were investigated using Mössbauer spectroscopy, X-ray diffraction, and transmission electron microscopy. In methanol, they consisted of $\alpha$-iron, $\gamma$-iron, iron carbide, and amorphous paramagnetic iron carbides, whereas in ethanol they consisted of iron carbides and amorphous paramagnetic iron carbides. The difference in products depending on the alcohol was attributed to the different carbon supplies for methanol and ethanol. For both solvents, the average particle size was found to be 16 nm, and the nanoparticles were dispersed in amorphous carbon. We also examined the effect of further laser irradiation of the colloids using stagnant solvent, and the particle size was found to increase and a very small amount of carbonization was observed.

**Keywords** Iron carbide · Nanoparticles · Laser ablation in liquid · Mössbauer spectroscopy

This article is part of the Topical Collection on *Proceedings of the 2nd Mediterranean Conference on the Applications of the Mössbauer Effect (MECAME 2016), Cavtat, Croatia, 31 May-3 June 2016*

✉ S. Amagasa
B115608@ed.tus.ac.jp

[1] Department of Chemistry, Tokyo University of Science, 1-3 Kagurazaka, Shinjuku-ku, Tokyo 162-8602, Japan

[2] Graduate School of Informatics and Engineering, The University of Electro-Communications, 1-5-1 Chofugaoka, Chofu, Tokyo 182-8585, Japan

[3] Nishina Center for Accelerator-Based Science, RIKEN, 2-1 Hirosawa, Saitama 351-0198, Japan

Published online: 25 July 2016

## 1 Introduction

Iron carbides have been studied extensively because of their applications to catalysis and magnetic materials. Iron carbide $Fe_5C_2$ nanoparticles were found to be an active phase for Fischer-Tropsch synthesis catalyst [1], and $Fe_3C$ nanoparticles encased by uniform graphitic layers catalyzed oxygen reduction [2]. The application of iron carbide nanoparticles as tunable magnetic hyperthermia materials has been reported [3]. Various iron carbides with different compositions and structures, such as ferrite, austenite, martensite, cementite $Fe_3C$, Hägg carbide $Fe_5C_2$ and Eckstrom-Adcock carbide $Fe_7C_3$ have been reported. Mössbauer spectroscopy is a useful and powerful tool for characterizing the properties of these compounds. Recently, iron carbon composites have received renewed attention because iron was found to catalyze the synthesis of carbon nanotubes [4, 5]. Various methods to produce iron carbide nanoparticles have been reported, such as laser pyrolysis [6], ball milling [7, 8], sonochemistry [9], and the polyol method [10].

Laser ablation synthesis in solution (LASiS) is the conventional method for producing nanoparticles [11] without the need for expensive chemicals and a large-scale apparatus. Iron carbide nanoparticles produced using laser ablation of an iron target in an organic solvent have been reported [12, 13]; however, in those studies, the laser ablation was conducted in a vessel open to the atmosphere, and the particles underwent oxidization by the oxygen dissolved in the solvent. In order to prevent such oxidation, we reported a synthesis of iron carbide nanoparticles employing an airtight vessel and degassed solvents [14].

With the laser ablation technique, laser irradiation of the metal target generates plasma vapor, and the vaporized metal atoms react with solvent molecules and condense rapidly to produce particles. Metastable particles are produced by the rapid quenching of highly excited states, and the metastable phase may stabilize as a result of large surface effects of the nanoparticles. However, the reaction mechanism for this process is not well understood. Further laser irradiation of a nanoparticle colloid promotes aggregation [15, 16].

In this study, in order to reduce the effects of laser irradiation on the suspended particles, we prepared iron carbide nanoparticles via the laser ablation of iron in a circulating solvent flow of either methanol or ethanol while simultaneously filtering out the products. We investigated the difference in products formed depending on the alcohol used and the effects of further laser irradiation of the colloids using stagnant solvent.

## 2 Experimental

A new cell consisting of an airtight vessel, a cellulose acetate filter (pore size: 0.45 $\mu$m), a three-necked flask and a diaphragm pump was developed for synthesizing nanoparticles using laser ablation (Fig. 1a). Prior to use, 200 mL of solvent (methanol or ethanol) was degassed and transferred to the airtight vessel. An iron block ($^{57}$Fe enriched) was placed in the solvent, and argon gas was introduced above the surface of the solvent to prevent oxidation in the vessel. The pressure of the vessel was kept at the atmospheric pressure by using a balloon attached to the three-necked flask. Laser ablation was performed for 60 minutes using a Nd:YAG laser (Continum, Surelite I-10; $\lambda = 532$ nm; repetition rate: 10 Hz; pulse energy: 150 mJ). The laser beam was introduced through a convex lens directly attached to the glass vessel. During the laser irradiation, the solvent was circulated at a flow rate of 0.45 L/min using the diaphragm pump. The nascent particles were collected on the filter, and were investigated using Mössbauer spectroscopy (Wissel, MDU1200, $^{57}$Co/Rh

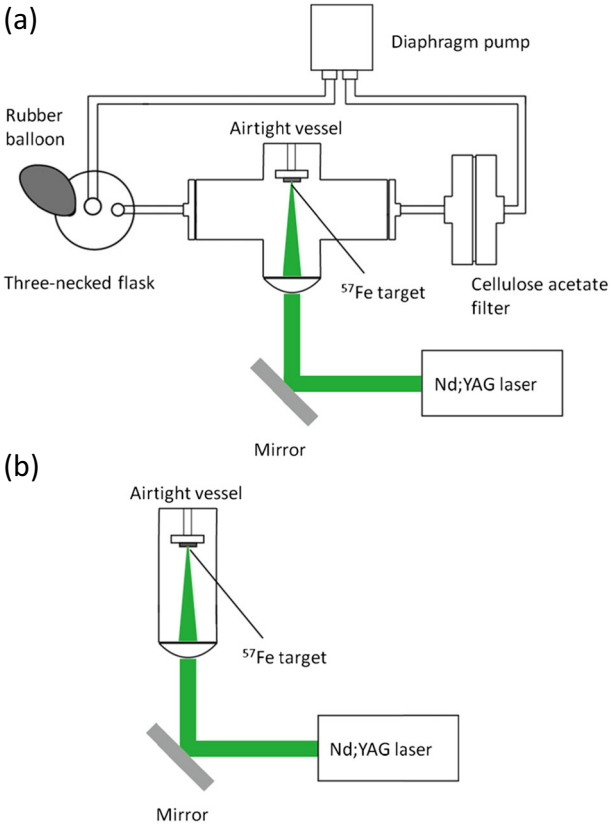


**Fig. 1** The schematic of the experimental setup. **a** The cell with a circulating solvent, and **b** the cell with a stagnant solvent

source), X-ray diffraction (XRD; Rigaku, RINT2000, Cu-K$\alpha$, operated at 50 kV/300 mA), and transmission electron microscopy (TEM; JEOL, JEM-2100, operated at 200 kV).

We also investigated the effects of further laser irradiation of the nanoparticle colloids. To do so, similar experiments to those described above were conducted using an airtight vessel without the pump and the filter (Fig. 1b). Laser ablation was performed in a stagnant solvent for 270 minutes under the same irradiation conditions, and the products were subsequently collected by centrifugation.

## 3 Results and discussion

TEM images of the nanoparticles produced in methanol and ethanol are shown in Fig. 2a and b, respectively, from which it can be seen that the particles were spherical and formed in large regions of amorphous carbon. The particle size distributions presented in Fig. 3 show that, in both solvents, the particles ranged from 1–40 nm in size (average size: 16 nm). Mössbauer spectra of the particles measured at 293 K are presented in Fig. 4, and their Mössbauer parameters are summarized in Table 1. The Mössbauer spectrum of the sample

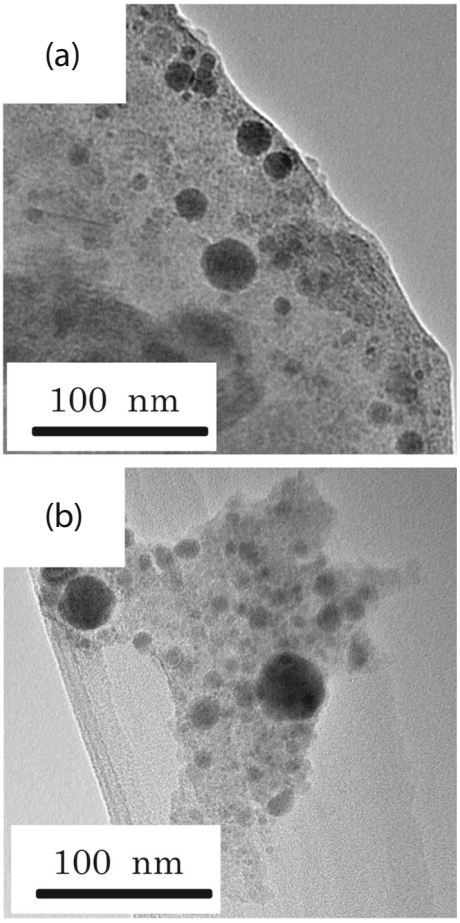


**Fig. 2** TEM images of nanoparticles produced in **a** methanol and **b** ethanol using the vessel equipped with the circulation system

produced in methanol (Fig. 4a) was fitted to a combination of a singlet, a doublet, and three sextets. The singlet was assigned to $\gamma$-Fe based on the isomer shift $\delta$, and the paramagnetic doublet was assigned to amorphous iron carbide. The magnetic components appeared as a broad absorption, indicating that the absorption peak consisted of a combination of several components. The most intense sextet was assigned to cementite $Fe_3C$ ($H = 20$ T), and the sextet exhibiting the largest hyperfine magnetic field was assigned to $\alpha$-Fe ($H = 33$ T). The remaining component was fitted to a sextet ($\delta = 0.18$ mm s$^{-1}$, $\Delta \boldsymbol{E}_q = -0.01$ mm s$^{-1}$, $H = 26$ T) with a relatively large peak width $\Gamma = 1.10$ mm s$^{-1}$. Although several types of iron carbides other than $Fe_3C$ have been reported, such as Hägg carbide ($Fe_5C_2$) and Eckstrom-Adcock carbide ($Fe_7C_3$) [6], the Mössbauer parameters for these iron carbides did not fit the sextet obtained in our experiments. Therefore, this spectral component was assigned to a "Fe-C alloy" previously reported in the literature [8], which consists of a metal iron lattice containing a small amount of carbon atoms and has a smaller hyperfine magnetic field than that for $\alpha$-Fe as well as a large line width.

As can be seen from Fig. 4b, the shape of the Mössbauer spectrum of the sample produced in ethanol was very different from that of the sample produced in methanol. The spectrum was fitted to a combination of a doublet and three sextets.

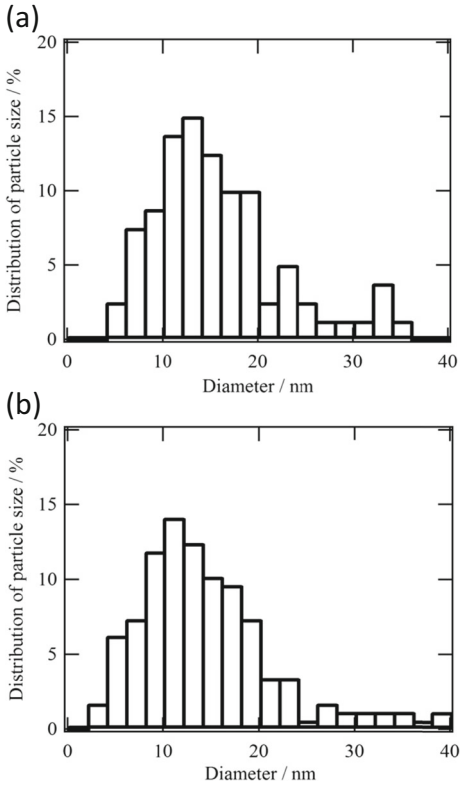


**Fig. 3** Size distribution of nanoparticles produced in **a** methanol and **b** ethanol using the vessel equipped with the circulation system

**Table 1** Mössbauer parameters of the spectra shown in Fig. 4

| Sample | Component | $\delta$ mm s$^{-1}$ | $\Delta E$q mm s$^{-1}$ | $H$ T | $\Gamma$ mm s$^{-1}$ | Yields % |
|---|---|---|---|---|---|---|
| (a) methanol | $\gamma-$iron | −0.05(0) | | | 0.33(2) | 5.9 |
| | amorphous | 0.03(0) | 0.71(1) | | 0.66(1) | 27.8 |
| | $Fe_3C$ | 0.18(1) | 0.02(1) | 20.0(1) | 0.92(2) | 38.7 |
| | Fe-C alloy | 0.18(1) | −0.01(2) | 26.2(1) | 1.02(6) | 22.5 |
| | $\alpha-$iron | 0.00* | 0.00* | 33.0* | 0.81(15) | 5.1 |
| (b) ethanol | amorphous | 0.20(0) | 1.08(1) | | 0.48(1) | 7.1 |
| | $Fe_3C$ | 0.18(0) | 0.02(0) | 20.7(0) | 0.59(1) | 30.7 |
| | $Fe_7C_3$ | 0.16(0) | −0.00(1) | 16.7(1) | 0.97(2) | 25.6 |
| | Fe-C alloy | 0.20(1) | −0.10(1) | 25.4(0) | 1.23(2) | 36.6 |

*Parameter were fixed in the fitting procedure

The $\gamma$-Fe singlet mentioned above was not present in the ethanol spectrum, and the doublet assigned to amorphous iron carbide was less intense. The magnetic components also appeared as a broad absorption peak, but had a different shape compared

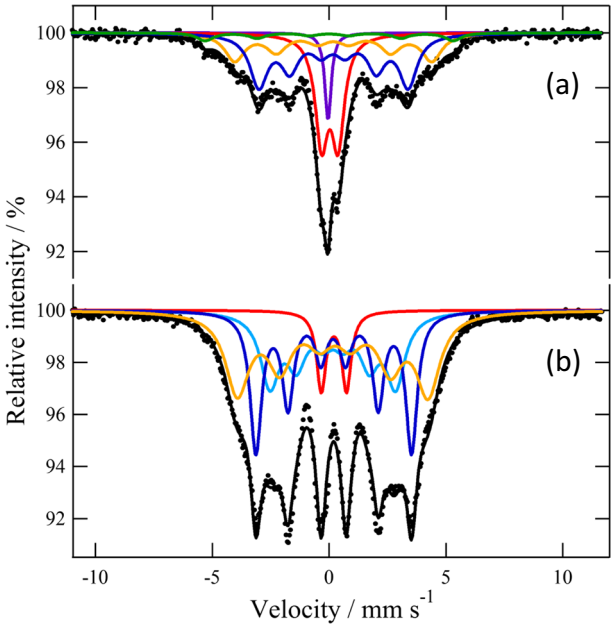


**Fig. 4** Mössbauer spectra of nanoparticles produced in **a** methanol and **b** ethanol using the vessel equipped with the circulation system. The spectra were measured at 293 K

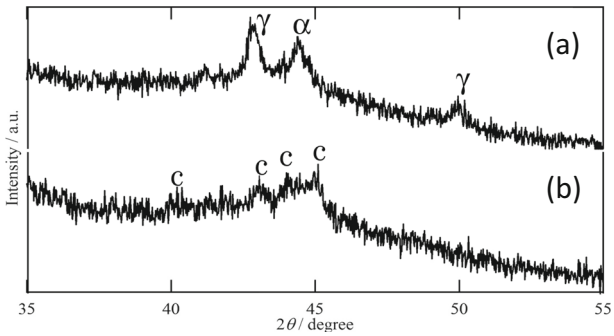


**Fig. 5** XRD patterns for the particles produced in **a** methanol and **b** ethanol using the vessel equipped with the circulation system. The labels $\gamma$, $\alpha$, and c correspond to $\gamma$-Fe (PDF #04-003-1443), $\alpha$-Fe (PDF #00-006-0696), and $Fe_3C$ (PDF #00-035-0772), respectively

to the methanol case. The most intense sextet was assigned to cementite $Fe_3C$ ($H$ = 21 T), which had a smaller line width due to the higher crystallinity of the particles. The intensity of the sextet assigned to Fe-C alloy ($H$ = 25 T) was higher, and the $\alpha$-Fe sextet was not observed. The remaining sextet with a smaller hyperfine magnetic field was assigned to $Fe_7C_3$. Although $Fe_7C_3$ was reported to have several

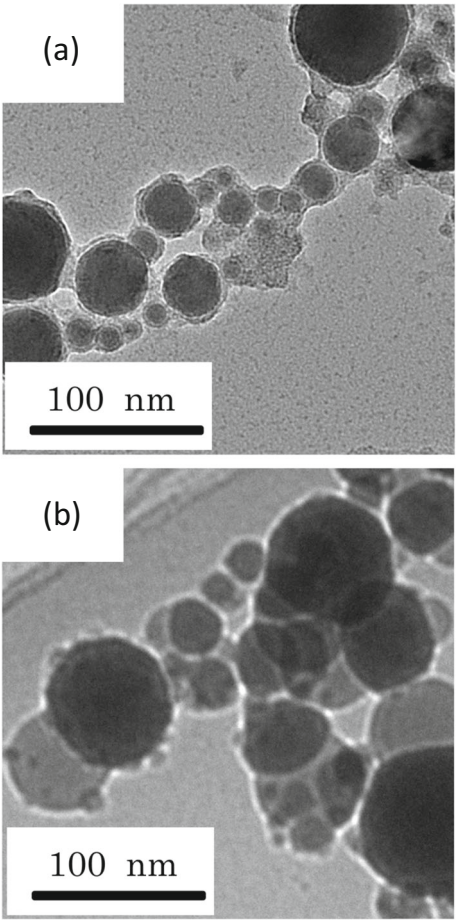


**Fig. 6** TEM image of particles produced in **a** methanol and **b** ethanol using the airtight vessel without solvent circulation

sites having closer Mössbauer parameters [6], the absorption was fitted to a sextet with a larger line width because it was not possible to resolve the sites in our spectrum.

Metallic $\alpha$-Fe and $\gamma$-Fe were observed only in the particles produced in methanol. A decrease in amorphous iron carbide and the increase in the iron carbides $Fe_3C$, Fe-C alloy, and $Fe_7C_3$ were observed in the particles produced in ethanol. The carbonization of iron was clearly enhanced in ethanol compared to in methanol. These differences can be attributed to the different carbon supplies for the two solvents. Upon decomposition in the plasma reaction field, an ethanol molecule supplies two times the amount of carbon atoms of a methanol molecule. As a result, carbon-rich phases were obtained in the particles produced in ethanol.

As can be seen in Fig. 5a, the XRD pattern for the sample produced in methanol exhibited $\alpha$-Fe and $\gamma$-Fe peaks, in agreement with the Mössbauer spectrum. The amorphous component was not observed in the XRD pattern. In addition, peaks corresponding to $Fe_3C$ or other iron carbides were not observed in the XRD pattern, as the crystallinity of the iron carbide crystals was too low to exhibit the long-range ordering detected by XRD. In contrast, as can be seen in Fig. 5b, the XRD pattern for the sample produced in ethanol exhibited

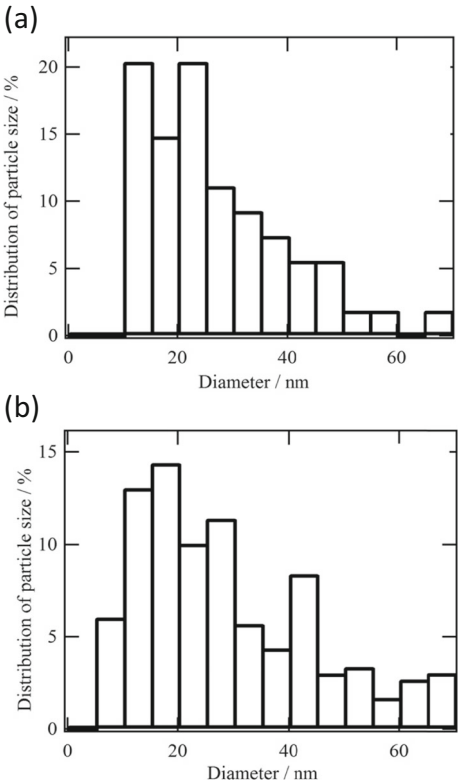


**Fig. 7** Size distribution of nanoparticles produced in **a** methanol and **b** ethanol using the airtight vessel without solvent circulation

only peaks corresponding to $Fe_3C$, in agreement with the Mössbauer spectrum. The $Fe_3C$ peak appeared because of the higher crystallinity of the particles produced in ethanol. The peaks corresponding to $Fe_7C_3$ and other iron carbides were not observed in the XRD pattern, as the crystallinity of the iron carbides was too low to exhibit the long-range ordering detected by XRD. In previous reports [12, 13], iron oxide nanoparticles were observed following laser ablation of iron in ethanol. In contrast, iron oxide production was not observed in the present study because the dissolved oxygen in the solvent was removed and exposure to the atmosphere was restricted.

In the experiments described above, the influence of laser irradiation on the nanoparticle colloids was intentionally limited by carrying out the ablation in a circulating solvent. In order to clarify the influence of laser irradiation on the nanoparticle colloids, similar experiments were conducted without employing the cell equipped with a pump. Instead, using an airtight vessel and a stagnant solvent, laser ablation was carried out for 270 min, and the particles were collected by centrifugation. Thereby, the nanoparticles were subjected to laser irradiation following their formation.

As shown in Fig. 6a and b, TEM images revealed that the sizes of the spherical particles increased as a result of the additional irradiation. The particle size distributions shown in Figs. 7a and b for methanol and ethanol, respectively, show that the additional irradiation led to enhanced aggregation and a widening of the distributions. The average sizes of the particles were 28 nm and 32 nm, respectively, for methanol and ethanol. The amorphous carbon observed in the TEM images of the particles produced in the solvent flows (Fig. 2)

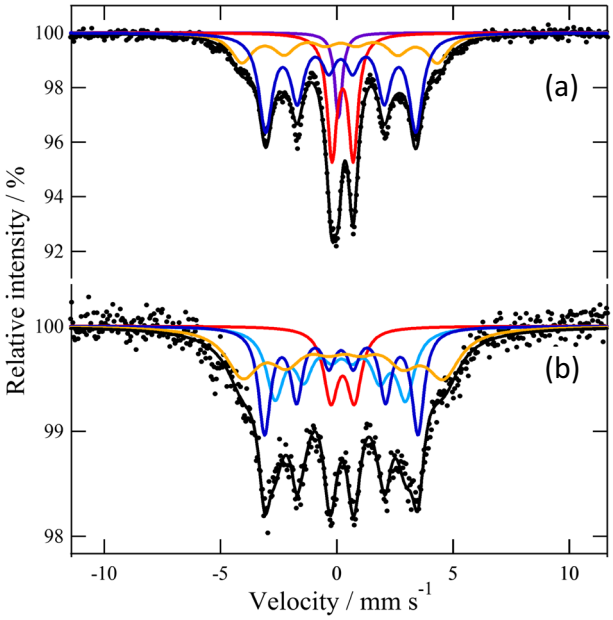


**Fig. 8** Mössbauer spectra of nanoparticles produced in **a** methanol and **b** ethanol using the airtight vessel without solvent circulation. The spectra were measured at 293 K

was not dominant in the TEM images of the particles produced in the stagnant solvents (Fig. 6).

Figure 8 shows Mössbauer spectra measured at 293 K of the particles produced using the airtight vessel and a stagnant solvent, and the Mössbauer parameters are summarized in Table 2. The effects of laser irradiation on the particles were clearly observed for the particles produced in methanol (Figs. 4a and 8a). Although the yield of $Fe_3C$ increased at the expense of $\alpha$-Fe and amorphous iron-carbon, the change in the chemical compositions of the nanoparticles was small. The laser irradiation of the colloids led to enhanced aggregation and lattice formation, while the effect on carbonation was relatively small. The difference in the Mössbauer spectra of the particles produced in ethanol (Figs. 4b and 8b) was very small, showing that the chemical composition did not change and that only the nanoparticle aggregation was enhanced by the laser irradiation of the colloids.

**Table 2** Mössbauer parameters of the spectra shown in Fig. 8

| Sample | Component | $\delta$ mm s$^{-1}$ | $\Delta Eq$ mm s$^{-1}$ | $H$ T | $\Gamma$ mm s$^{-1}$ | Yields % |
|---|---|---|---|---|---|---|
| (a) methanol | $\gamma-$iron | 0.07(0) | | | 0.38(2) | 6.0 |
| | amorphous | 0.25(0) | 0.91(1) | | 0.50(1) | 22.3 |
| | $Fe_3C$ | 0.17(0) | −0.00(1) | 20.1(0) | 0.70(1) | 48.8 |
| | Fe-C alloy | 0.15(1) | −0.05(2) | 26.2(1) | 1.10(5) | 22.9 |
| (b) ethanol | amorphous | 0.25(2) | 1.01(3) | | 0.75(7) | 11.4 |
| | $Fe_3C$ | 0.19(1) | 0.01(2) | 20.5(1) | 0.63(9) | 28.6 |
| | $Fe_7C_3$ | 0.18(2) | −0.06(4) | 17.5(3) | 0.91(34) | 26.4 |
| | Fe-C alloy | 0.31(5) | −0.07(8) | 26.8(4) | 1.70(15) | 33.6 |

## 4 Conclusion

Spherical particles 16 nm in diameter were produced by laser ablation of iron metal in a flow of either methanol or ethanol. By circulating the solvent, the influence of further laser irradiation of the colloids that is unavoidable when using a stagnant solvent was eliminated. The particles produced in methanol consisted of metallic iron ($\alpha$-Fe and $\gamma$-Fe) and iron carbides (mainly $Fe_3C$), while the particles produced in ethanol consisted of iron carbides. This difference can be attributed to the different carbon atom supplies for ethanol and methanol: an ethanol molecule supplies two times more C atoms than a methanol molecule. Laser ablation was also performed in a stagnant solvent to investigate the effect of laser irradiation on the nanoparticle colloids. Laser irradiation was found to induce aggregation, approximately doubling the particle sizes to $\sim$30 nm, but no significant change in the chemical identity of the particles was observed.

**Acknowledgments** This work was supported by JSPS KAKENHI Grant Number JP16K05733.

## References

1. Yang, C., Zhao, H., Hou, Y., Ma, D.: $Fe_5C_2$ Nanoparticles: A Facile Bromide-Induced Synthesis and as an Active Phase for Fischer−Tropsch Synthesis. J. Am. Chem. Soc. **134**, 15814–15821 (2012)
2. Hu, Y., Jens, O.J., Zhang, W., Cleemann, L.N., Xing, W., Bjerrum, N.J., Li, Q.: Hollow spheres of iron carbide nanoparticles encased in graphitic layers as oxygen reduction catalysts. Angew. Chem. Int. Ed. **53**, 3675–3679 (2014)
3. Meffre, A., Mehdaoui, B., Kelsen, V., Fazzini, P.F., Carrey, J., Lachaize, S., Respaud, M., Chaudret, B.: A Simple Chemical Route toward Monodisperse Iron Carbide Nanoparticles Displaying Tunable Magnetic and Unprecedented Hyperthermia Properties. Nano. Lett. **12**, 4722–4728 (2012)
4. Pérez-Cabero, M., Taboada, J.B., Guerrero-Ruiz, A., Overweg, A.R., Rodríguez-ramos, I.: The role of alpha-iron and cementite phases in the growing mechanism of carbon nanotubes: a $^{57}$fe mössbauer spectroscopy study. Phys. Chem. Chem. Phys. **8**, 1230–1235 (2006)
5. Yoshida, H., Takeda, S., Uchiyama, T., Kohno, H., Homma, Y.: Atomic-scale In-situ Observation of Carbon Nanotube Growth from Solid State Iron Carbide Nanoparticles. Nano. Lett. **8**(7), 2082–2086 (2008)
6. Bi, X., Ganguly, B., Huffman, G., Huggins, F., Endo, M.: Nanocrystalline $\alpha-$Fe, $Fe_3C$, and $Fe_7C_3$ produced by $CO_2$ laser pyrolysis. J. Mater. Res. **8**(7), 1666–1674 (1993)
7. Tanaka, T., Nasu, S., Ishihara, K.N., Shingu, P.H.: Mechanical alloying of the high carbon Fe-C system. J. Less-Common Metals **171**, 237–247 (1991)
8. Miani, F., Matteazzi, P., Basset, D.: Mechanosynthesis of iron carbides at composition $Fe_{75}C_{25}$: modeling of the process kinetics. J. Alloys and Compounds **204**, 151–156 (1994)
9. Miyatani, R., Yamada, Y., Kobayashi, Y.: Mössbauer study of iron carbide nanoparticles produced by synthesis. J. Radioanal. Nucl. Chem. **330**(2), 1503–1506 (2015)
10. Yamada, Y., Shimizu, R., Kobayashi, Y.: Iron oxide and iron carbide particles produced by the polyol method. Hyperfine Interact. **237**, 6 (2016)
11. Mafuné, F., Kohno, J., Takeda, Y., Kondow, T.: Formation and size control of silver nanoparticles by laser ablation in aqueous solution. J. Phys. Chem. B **104**, 9111–9117 (2000)
12. Amendola, V., Riello, P., Meneghetti, M.: Magnetic nanoparticles of iron carbide, iron oxide, Iron@Iron oxide, and metal iron synthesized by laser ablation in organic solvents. J. Phys. Chem. C **115**, 5140–5146 (2011)
13. Franzel, L., Bertino, M.F., Huda, Z.J., Carpenter, E.E.: Synthesis of magnetic nanoparticles by pulsed laser ablation. Appl. Surf. Sci. **261**, 332–336 (2012)
14. Matsue, T., Yamada, Y., Kobayashi, Y.: Iron carbide nanoparticles produced by laser ablation in organic solvent. Hyperfine Interact. **205**, 31–35 (2012)
15. Niidome, Y., Hori, A., Sato, T., Yamada, S.: Enormous size growth of Thiol-passivated gold nanoparticles induced by near-IR laser light. Chem. Lett. **29**(4), 310–311 (2000)
16. Tsuji, T., Yahata, T., Yasutomo, M., Tsuji, M., Igawa, K., Ishikawa, Y., Koshizaki, N.: Preparation and investigation of the formation mechanism of submicron-sized spherical particles of gold using laser ablation and laser irradiation in liquids. Phys. Chem. Chem. Phys. **15**, 3099–3107 (2013)